DØ Hot Topics

D. Buchholz on behalf of the DØ Collaboration
Northwestern University, Department of Physics and Astronomy, Evanston, Il 60208, USA

We present recent DØ results based on approximately 1 fb^{-1} of $p\bar{p}$ collisions at $\sqrt{s}$ = 1.96 TeV recorded at the Fermilab Tevatron. Preliminary results on a search for the flavor changing neutral current process $D^+ \to \pi^+\mu^+\mu^-$, a measurement of the CP violation parameter in B mixing, ϵ_B, and a two sided limit on the B_s oscillation frequency Δm_s are presented. The limits on ϵ_B and $\mathcal{B}(D^+ \to \pi^+\mu^+\mu^-)$ are the world's best limits. The two sided bound on Δm_s is the first direct indication by a single experiment that Δm_s is bounded from above.

1. Introduction

A major goal of the heavy flavor physics community is to find indirect evidence of new physics by studying neutral meson mixing and flavor changing neutral current (FCNC) decays. In the Standard Model (SM) these processes are mediated by higher order weak transitions and can receive sizeable corrections from new particles as predicted by several extensions to the SM. These new physics corrections are manifested in either an augmentation of the decay or mixing rate, or possibly by introducing new complex operators leading to unexpected sources of CP violation.

The DØ experiment operating at the Fermilab Tevatron has a rich heavy flavor program built on the excellent performance of the DØ muon system. The large single and dimuon data samples are ideal for studying heavy flavor mixing and radiative decay. In this presentation, we focus on three results that highlight the strengths of the program: a search for the flavor changing neutral current transition $c \to u\mu^+\mu^-$ [1], a search for CP violation in B mixing [2], and our progress in measuring the B_s mixing frequency [3]. These results are derived from a data sample of $p\bar{p}$ collisions at $\sqrt{s} = 1.96$ TeV corresponding to a luminosity of approximately 1 fb^{-1}.

2. DØ experiment

The DØ detector is a general purpose spectrometer and calorimeter [4]. Charged particles are reconstructed using a silicon vertex tracker and a scintillating fiber tracker located inside a superconducting solenoid coil that provides a 2 T magnetic field. Photons and electrons are reconstructed using the inner region of a liquid argon calorimeter optimized for electromagnetic shower detection. Jet reconstruction and electron identification are further augmented with the outer region of the calorimeter optimized for hadronic shower detection. Muons are reconstructed using a spectrometer consisting of magnetized iron toroids and three super-layers of proportional tubes and plastic trigger scintillators located outside the calorimeter.

The DØ trigger is based on a three tier system. The level 1 and 2 dimuon triggers rely on energy deposited in the muon spectrometer and fast reconstruction of muon tracks. For single muon triggers the muon is required to be associated with a track in the central detector with a transverse momentum of at least 3 GeV/c. The level 3 trigger performs fast reconstruction of the entire event allowing for further muon identification algorithms, improved matching of muon candidates to tracks reconstructed in the central tracking system, and requirements on the z position of the primary vertex. At higher luminosities, we increase the penetration requirements on the dimuon triggers, the momentum thresholds are usually raised to as high as 5 GeV/c on the single muon triggers, and invariant mass or displaced particle filters are added at level 3 to enhance the heavy flavor content of the muon samples.

3. Flavor Changing Neutral Current Charm Decays

The excellent agreement between observed FCNC processes involving down-type charge $-1/3$ quarks such as $b \to s\gamma$, $b \to sl^+l^-$, and $K \to \pi\nu\bar{\nu}$ with SM expectations have been used to set strict limits on new phenomena [5–7]. However, there are several scenarios of new phenomena such as SUSY R parity violation in a single coupling scheme [7], or little Higgs models with a new up-like vector quark [8] where deviations from the SM would only be seen in the up sector. Scenarios of this nature motivate the study of FCNC charm meson decays.

Due to GIM suppression, the SM rates for FCNC charm decays vanish in the limit of SU(3) symmetry. The inclusive rates of decays such as $D^+ \to \pi^+l^+l^-$ are therefore expected to be dominated by long distance contributions where the dilepton system is produced via intermediate strong resonances such as the ϕ or the ω [9, 10]. Of particular interest is the decay $D_s^+ \to \pi^+\mu^+\mu^-$ that can only proceed via the long distance interaction where the dimuon system is produced by an intermediate ϕ meson. Since this has no short distance contributions, the rate is given

simply by the product of the two branching fractions of $D_s^+ \to \phi\pi^+$ and $\phi \to \mu^+\mu^-$. Just as the decay $B^+ \to J/\psi K^+ \to K^+l^+l^-$ played a crucial role in benchmarking the studies of $b \to sl^+l^-$ transitions, the observation of the Cabbibo favored decay $D_s^+ \to \phi\pi^+ \to \pi^+l^+l^-$ is an essential first step in the study of $c \to ul^+l^-$ transitions. Once this mode has been observed, the search for continuum production of $c \to ul^+l^-$ can be performed by looking for an excess of D^+ candidates where the dilepton mass is inconsistent with resonance production.

D meson candidates are formed by combining two well reconstructed muons with a track in the same jet as the dimuon system and requiring the three particle system have an invariant mass consistent with a D meson. If multiple candidates exist for a single event, the best candidate is selected based on the quality of the three track vertex, the transverse momentum of the pion, and the radial distance between the pion and the dimuon system. Backgrounds from light quarks or random combinations are reduced further with variables that take advantage of the long D meson lifetime and distinct decay topology.

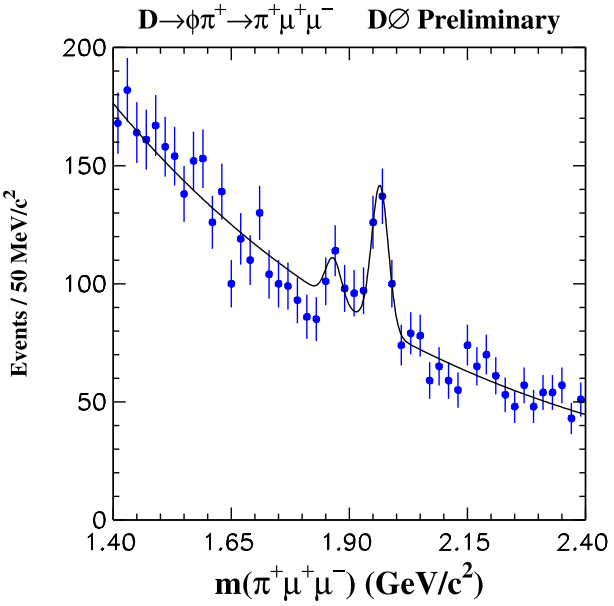

Figure 1: The $m(\pi^+\mu^+\mu^-)$ mass spectrum for the loose cut sample in the $0.96 < m(\mu^+\mu^-) < 1.06$ GeV/c^2 bin. The results of binned likelihood fits to the distributions including contributions for D_s^+, D^+, and combinatoric background are overlaid on the histogram.

The first goal is to observe the resonance production of $D_s \to \phi\pi \to \pi\mu^+\mu^-$. The D meson candidates for events where the dimuon system has an invariant mass consistent with a ϕ meson are shown in Fig 1 for loose selection requirements and in Fig 2 for requirements optimized for resonance production and background suppression. In both plots a D_s signal is clearly observed and in the optimized selection the D^+ signal is also seen with a significance above background of 3.1 sigma. From this we extract the branching fraction

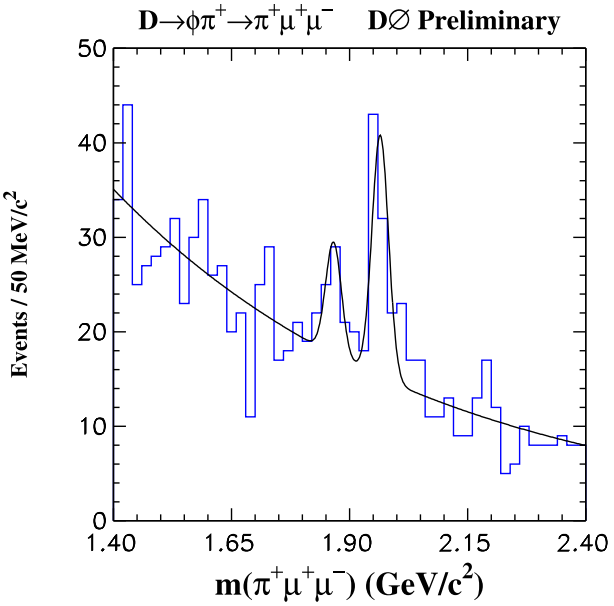

Figure 2: The $m(\pi^+\mu^+\mu^-)$ mass spectrum for the optimized D_s^+ sample in the $0.96 < m(\mu^+\mu^-) < 1.06$ GeV/c^2 bin. The results of binned likelihood fits to the distributions including contributions for D_s^+, D^+, and combinatoric background are overlaid on the histogram.

$$\mathcal{B}(D^+ \to \phi\pi^+ \to \pi^+\mu^+\mu^-) = (1.75 \pm 0.7 \pm 0.5) \times 10^{-6}$$

which can be compared to the recent CLEO-c measurement of $(2.7^{+3.6}_{-1.8} \pm 0.2) \times 10^{-6}$ or the expected value of 1.77×10^{-6} given by the product of the $D^+ \to \phi\pi^+$ and the $\phi \to \mu^+\mu^-$ branching fractions.

Having clearly established the resonance production, we turn to a search for non resonant D production. The D meson candidates for events passing tight requirements optimized for the non resonant analysis are shown in Fig 3. The distribution on the left are again events where the dimuon system has an invariant mass consistent with a ϕ meson. We expect to still see some excess from the D_s and $D^+ \to \phi\pi^+$ signals and indeed based on the yields from the above sample we predict 5.3 ± 1.5 events (signal plus background) in the D^+ signal region and 4.6 ± 0.7 events in the D_s signal region which compare well to the observed 6 events in the D^+ window and 3 events in the D_s window. This indicates that even after the tighter selection we still have sensitivity at the level of the D^+ branching fraction measured above.

The distribution in Fig 4 shows the D candidates where the dimuon system has an invariant mass outside the ϕ window. Here we see 17 events in the D^+ window that are consistent with the expected background of 20.9 ± 3.4 events. From this, we set the

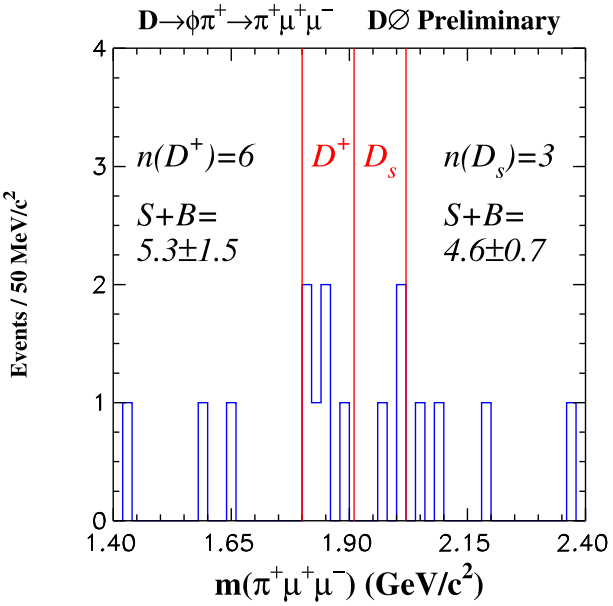

Figure 3: The $m(\pi^+\mu^+\mu^-)$ mass spectrum for the optimized D^+ sample in the $0.96 < m(\mu^+\mu^-) < 1.06$ GeV/c^2 bin. The line is a fit to the data in the sideband regions $1.4 < m(\pi^+\mu^+\mu^-) < 1.7$ GeV/c^2 and $2.1 < m(\pi^+\mu^+\mu^-) < 2.4$ GeV/c^2. The D^+ and D_s^+ signal yields are fixed based on the yields in the optimized D_s^+ sample and the relative efficiencies between the D_s^+ and D^+ cuts.

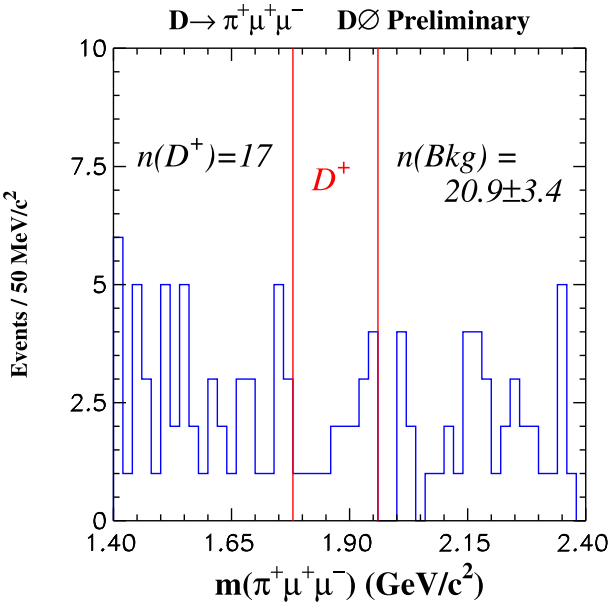

Figure 4: Final search for $D^+ \to \pi^+\mu^+\mu^-$ in the continuum region.

90% confidence level upper limit

$$\mathcal{B}(D^+ \to \pi^+\mu^+\mu^-) < 4.7 \times 10^{-6}.$$

This is the most stringent limit to date in the dimuon modes. Although this is approximately 500 times above the SM expected signal it is already below the allowed parameter space of SUSY R parity violating couplings.

4. CP Violation in B Mixing

The CP eigenstates of neutral B mesons are a linear combination of the flavor eigenstates

$$B_{CP} = pB^0 + q\bar{B}^0.$$

A difference in the coefficients $q \neq p$ would lead to CP violation B mixing. The signature of B mixing is like-sign dilepton events indicating that the initially produced $B\bar{B}$ system decayed as either a BB or a $\bar{B}\bar{B}$ combination. The experimental signature for CP violation in B mixing would be an asymmetry between the number of l^+l^+ and l^-l^- final states.

Since the current experimental limits are slightly below the percent level, our goal is to measure the charge asymmetry between like-sign dimuons at the tenth percent level precision.

At DØ , we can reach the desired accuracy by taking advantage of the two independent magnetic spectrometers: the inner solenoid and the outer muon system toroid. The field polarities are reversed frequently leading to roughly equal data sets with the four possible combinations of field configurations. Comparing yields in these data sets allows us to make precise determinations of all detector induced asymmetries.

The raw event yields for different combined toroid solenoid polarities are listed in Table I for our 1 fb^{-1} data set. The like-sign dimuon asymmetry after removing detector effects is

$$A = -0.0013 \pm 0.0012 \pm 0.0008.$$

To extract the underlying CP violating semileptonic asymmetry A_{SL} from this number requires precise knowledge of the composition of our dimuon sample. Besides our signal of direct semileptonic decay of both b hadrons in the event, an important component of the sample is the coincidence of a primary muon from semileptonic b decay and a secondary muon from semileptonic charm decay. Topologies like these that produce like-sign dimuons but are not associated with B mixing dilute the asymmetry.

Table I Raw Results.

Toroid*Solenoid Polarity	-1	+1
N++	177,950	156,183
N– –	176,939	156,148
N+ –	1,175,547	1,029,604

The most problematic component are asymmetries induced by hadronic interactions of kaons in the detector. Reactions like $K^- + N \to \Lambda\pi$ have no K^+ analog. As the kaons travel through the detector the fraction of K^+ increases and leaving a larger number of μ^- from K^+ decay in flight than μ^+ from K^- decay in flight. We measure this asymmetry directly from reconstructed $B \to D^*\mu\nu$ events in the data sample and subtract it from the above asymmetry. This is by far the largest source of systematic error in the analysis.

A sensitive cross check of the sample composition is the extraction of the integrated B mixing probability χ that can be extracted from the ratio of like-sign dimuons to opposite-sign dimuons. In our data set we find

$$\chi = 0.136 \pm 0.001 \pm 0.024.$$

This can be compared to the Particle Data Group (PDG) [11] value of $\chi(\mathrm{PDG}) = 0.1281 \pm 0.0076$. With our knowledge of the sample composition, we can then extract from the raw asymmetry the semileptonic asymmetry

$$A_{SL} = -0.0044 \pm 0.0040 \pm 0.0028.$$

From which we extract the CP violation in B mixing parameter ϵ_B

$$\frac{\mathcal{R}(\epsilon_B)}{1 + |\epsilon_B|^2} = -0.0011 \pm 0.0010 \pm 0.0007.$$

This measurement gives the best sensitivity to CP violation in B mixing to date and can be compared to the world average value of all previous measurements (0.0005 ± 0.0031) [11].

5. B_s Mixing

Measurements of flavor mixing in neutral meson systems have historically led to profound insights into physics at energy scales inaccessible to particle accelerators. The discovery of mixing and CP violation in the neutral kaon system [12] led Kobayashi and Maskawa to predict the existence of a third flavor generation [13]. The discovery of mixing in the B_d system gave the first indication that the top quark is much heavier than the W boson [14]. Finally, mixing induced CP violation measurements in the B_d system have precisely determined the phase of the CP violating top quark coupling $\mathrm{Arg}(V_{td}) \sim 24^\circ$ [15]. This motivates the study of mixing in the B_s system. A B_s mixing measurement allows a precise determination of the magnitude of the CP violating top coupling through the ratio $|V_{td}/V_{ts}|$ and may lead to the discovery of new physics in $b \to s$ transitions [16].

Measuring the B_s oscillation frequency requires knowledge of the B_s flavor at both production and decay. Signatures of mixing are candidates where the flavor at decay is different than the flavor at production. The mixing frequency can be determined by looking for an oscillation in the fraction of mixed events as a function of the B_s decay length.

The B_s flavor at decay is determined by reconstructing a flavor-specific final state. At DØ , we use the semileptonic decay $B_s^0 \to D_s^-\mu^+\nu$, $D_s^- \to \phi\pi^-$, $\phi \to K^+K^-$ and charge conjugate states. The $\phi\pi$ invariant mass distribution is shown in Fig 5. In our 1 fb^{-1} sample. we reconstruct approximately 26.7 thousand $D_s\mu$ candidates predominantly from B_s decay and 7.4 thousand $D^+\mu$ candidates predominantly from B^0 decay. The B_s flavor at production is determined by examining inclusive properties of the system recoiling against the B_s candidate. In this way, we determine the flavor of the other B hadron in the event that was pair produced with the B_s candidate. We use a likelihood based tagging algorithm based on momentum weighted sum of the charge of particles associated with either a lepton, a displaced vertex, or the entire recoil system. Fig 5b shows the event sample when the flavor tag is required. The tagging purity of the combined likelihood is determined event by event and is calibrated by studying B_d mixing in our $B_d^0 \to D^{*-}\mu^+\nu$ sample. The figure of merit for tagging is the effective efficiency, ϵD^2, that takes into account both the efficiency of the tagging algorithm and the weight that each event receives in the final analysis due to the purity of the tag. In our $D^*\mu\nu$ sample, we measure an effective efficiency of

$$\epsilon D^2 = 2.48 \pm 0.21^{+0.08}_{-0.06}.$$

The decay length of the B_s meson is taken as the transverse distance from the primary vertex reconstructed using tracks originating in the beam spot, and the secondary vertex reconstructed from the D_s and μ particles. To boost the decay length to the proper frame, we use MC to simulate the missing energy from the neutrino or other pions or kaons from $B_s \to D_sX$ decays.

We require a very accurate determination of our decay length resolution so that we can distinguish a lack of a signal in our data from a lack of the ability to resolve a frequency beyond our resolution. We test our resolution model using prompt J/ψ candidates from $p\bar{p} \to J/\psi X$ interactions. Here the J/ψ decays at the primary vertex so that our measurement of the distance from the primary vertex to the J/ψ vertex is a direct measurement of our resolution.

Fig 6 shows the value of $-\Delta log\mathcal{L}$ as a function of Δm_s, indicating a favored value of $19ps^{-1}$, while variations of -$log\mathcal{L}$ from the minimum indicates an oscillation frequency of $17 < \Delta m_s < 21ps^{-1}$ at the 90% C.L. The uncertainties are approximately Gaussian inside the interval. Using 1000 parameterized Monte Carlo

samples, it was determined that for a true value of $\Delta m_s = 19ps^{-1}$, the probability was 15% for measuring a value in the range $17 < \Delta m_s < 21ps^{-1}$ with a $-\Delta log\mathcal{L}$ lower by at least 1.9 than the corresponding value at $\Delta m_s = 25ps^{-1}$.

The amplitude method [17] was also used and the results are shown in Fig 7. The unbinned likelihood fit is repeated including the oscillation amplitude $\mathcal{A}$ as a function of the input value of Δm_s. At $\Delta m_s = 19ps^{-1}$ the measured data point deviates from the hypothesis $\mathcal{A} = 0$ ($\mathcal{A} = 1$) by 2.5 (1.6) standard deviations, corresponding to a two-sided C.L. of 1% (10%), and is in agreement with the likelihood results. This is the first report of a direct two-sided bound on the B_s^0 oscillation frequency.

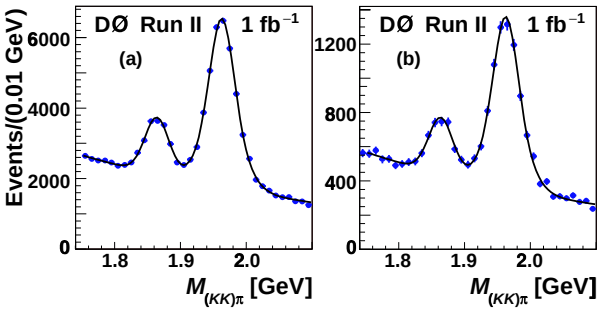

Figure 5: $(K^+K^-)\pi^-$ invariant mass distribution for (a) the untagged B_s^0 sample, and (b) for candidates that have been flavor-tagged. The left and right peaks correspond to μ^+D^- and $\mu^+D_s^-$ candidates, respectively. The curve is a result of fitting a signal plus background model to the data. For fitting the mass spectra, a single Gaussian function was used to describe the $D^- \to \phi\pi^-$ decays and a double Gaussian was used for the $D_s^- \to \phi\pi^-$ decays. The background was modeled by an exponential function.

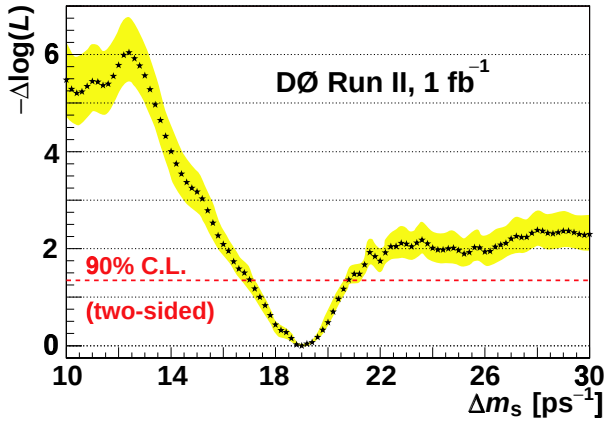

Figure 6: Value of $-\Delta log\mathcal{L}$ as a function of Δm_s. Star symbols do not include systematic uncertainties, and the shaded band represents the envelope of all $log\mathcal{L}$ scan curves due to different systematic uncertainties.

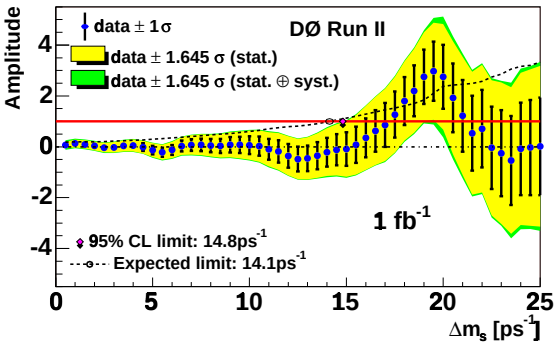

Figure 7: B_s^0 oscillation amplitude as a function of oscillation frequency, Δm_s.

6. Conclusions

DØ preliminary results based on approximately 1 fb^{-1} of $p\bar{p}$ collisions at $\sqrt{s} = 1.96$ TeV recorded at the Fermilab Tevatron have been presented. We set the most stringent limit to date in a search for the flavor changing neutral current in the dimuon modes. At the 90% confidence level upper limit we find $\mathcal{B}(D^+ \to \pi^+\mu^+\mu^-) < 4.7 \times 10^{-6}$. We have extracted the CP violation in B mixing parameter ϵ_B

$$\frac{\mathcal{R}(\epsilon_B)}{1 + |\epsilon_B|^2} = -0.0011 \pm 0.0010 \pm 0.0007,$$

which is the best sensitivity to CP violation in B mixing to date. We have presented the first report of a direct two-sided bound on the B_s^0 oscillation frequency, $17 < \Delta m_s < 21ps^{-1}$ at the 90% C.L.

References

[1] V.M. Abazov *et al.*, (DØ Collaboration) DØ Conference Note 5038, http://www-d0.fnal.gov

[2] V.M. Abazov *et al.*, (DØ Collaboration) DØ Conference Note 5042, http://www-d0.fnal.gov

[3] V.M. Abazov *et al.*, (DØ Collaboration) Fermilab-Pub-06/055-E, hep-ex/0603029, submitted to PRL.

[4] V.M. Abazov *et al.*, (DØ Collaboration) Fermilab-Pub-05/341-E, hep-physics/0507191, submitted to NIM-A.

[5] A.L. Kagen and M. Neubert, Eur. Phys. J. **C7**, 5 (1999).

[6] A. Ali, E. Lunghi, C. Greb, G. Hiller, Phys. Rev. **D66**, 034002 (2002).

[7] K. Agashe and M. Graesser,Phys. Rev. **D54**, 4445 (1996).

[8] S. Fajfer and S. Perlovsek, hep-ph/0511048

[9] G. Burdman, E. Golowich, J. Hewett, S. Pakvasa, Phys. Rev. **D66**, 014009 (2002).

[10] S. Fajfer, S. Prelovsek , P. Singer, Phys. Rev. **D64**, 114009 (2001).
[11] S. Eidelman *et al.*, Phys. Lett. **B592**, 1 (2004).
[12] J. H. Christenson *et al.*, Phys. Rev. Lett, **13**, 138 (1964).
[13] M. Kobayshi and T. Maskawa, Prog. Theor. Phys. **49**, 652 (1973).
[14] H. Albrecht *et al.*, (ARGUS Collaboration), Phys. Lett. **B192**, 245 (1987).
[15] Heavy Flavor Averaging Group, "Averages of b-hadron properties at the end of 2005," arXiv:hep-ex/0603030.
[16] "B Physics at the Tevatron: Run II and Beyond," arXiv:hep-ph/0201071.
[17] H.G. Moser and A. Roussarie, Nucl. Instr. Meth. **A384**, 491 (1997).